Robust entrainment phenomena of oscillations by delay time in the photosensitive Oregonator model

Wei Bao,[1] Zan Li,[1] Lu-Qun Zhou,[1,*] and Zhuo Gao[2]
[1]*State Key Laboratory for Mesoscopic Physics, Department of Physics, Peking University, Beijing 100871, China*
[2]*Physics Group, Institute of Chemical Defense, Beijing 102205, China*
(Received 23 March 2008; revised manuscript received 20 October 2008; published 23 January 2009)

The influences of delayed feedback on the oscillating behaviors are numerically investigated by using the photosensitive Oregonator model with a Hopf point. We find that the time delay in the robust entrainment phenomena determines the time scale of the system, that is, $T_m=(\tau+\delta)/N$ $(N=1,2,\cdots)$, where T_m is the mean period of the oscillation and δ is a small constant compared with the delay time τ. Further, our numerical simulation shows that, when the system has a characteristic period T_0 under the feedback with time delay, there exists an asymptotical line $\delta=\delta_0 T_0$ (δ_0 independent of any parameters) in the entrainment region with increasing strength of the feedback control c; when the system has no characteristic period, the above linear relation is also kept, and δ decreases with increasing c.

DOI: 10.1103/PhysRevE.79.016214 PACS number(s): 05.45.Xt, 82.40.Bj

I. INTRODUCTION

Delayed feedback is common to numerous biological [1], physiological [2], and electronic systems [3], and it may change the dynamic behavior of a system dramatically. It is well known that delayed feedback is one of the most efficient measures in enhancing the regularity of a system and can be used as a powerful method to control chaos or turbulence via stabilizing the unstable periodic orbits (UPOs) embedded in the chaotic attractor [4]. On the other hand, in a minimal bromate oscillator (MBO) system [5], a nonlinear delayed feedback controlling the flow rate of one reactant can cause Hopf bifurcation, period doubling, and bifurcation into chaos. A positive electrical feedback in the oscillating Belousov-Zhabotinsky (BZ) reaction is found to have an effect on the Hopf points [6].

The BZ reaction is one of the pioneering experimental systems for nonlinear dynamics and is widely used in research. The photosensitive ruthenium(II)-tris(bipyridine)-catalyzed BZ reaction is used to study spiral wave dynamics under feedback control [7] and frequency-locking phenomena of propagating wave fronts by changing the external illumination intensity [8]. The major dynamics is described by a set of differential equations known as the modified Oregonator accounting for the light sensitivity [9], which has a subcritical Hopf bifurcation when the light intensity is chosen as the bifurcation parameter. This mathematical model was used to demonstrate both stochastic resonance for weak-signal detection [10] and subthreshold firing under periodic perturbation [11,12].

Recently, time-delayed feedback was found to steer the time scales of noise-induced motion by changing the time delay, when it is used in coherence resonance oscillators [13]. A similar behavior was found by Balanov *et al.* [14], which shows that the characteristic features of noise-induced spatiotemporal patterns can be effectively controlled by applying delayed feedback. So there exists an important question: Is the effect of noise necessary for the entrainment phenomenon? In fact, such an entrainment phenomenon that the period of the controlled oscillations increases and decreases as a function of the time delay in a "sawtooth" fashion was also found in an oscillatory system without noise [15]. So we consider that in the noisy system the oscillations are sustained by noise and the mean interspike interval of a wave train is controlled by varying the time delay can be seen as two phenomena caused by two independent nonlinear mechanisms. In this paper, we numerically study the nonlinear dynamical behaviors of the Oregonator model with a Hopf point under the delayed feedback control. In the parameter space we observe four different dynamical behaviors and find that the state of the nonlinear system under feedback without delay and the original Hopf point of the system under no feedback can be used as hallmarks in predicting the dynamic behavior. Moreover, when the system has no characteristic period under feedback without time delay, the time scale of the system is almost determined by the time delay; in contrast, when the system has a characteristic period under feedback without time delay in the region, the time scale of the system is determined by the competition between the characteristic period and time delay. When the strength of the feedback is strong enough, the entrainment data asymptotically fit a perfect linear relation. Both cases demonstrate that the entrainment of an oscillator's period by time delay is quite robust.

II. MODEL

We use the photosensitive Oregonator model as follows [11]:

$$\epsilon_1 \frac{dx}{dt} = x(1-x) + y(q-x) - \epsilon_1 \kappa_f x + p_2 \Phi(t), \qquad (1)$$

$$\epsilon_2 \frac{dy}{dt} = 2hz - y(q+x) + \epsilon_2 \kappa_f (y_0 - y) + p_1 \Phi(t), \qquad (2)$$

*zhoulq@pku.edu.cn

$$\frac{dz}{dt} = x - z - \kappa_f z + \left(\frac{p_1}{2} + p_2\right)\Phi(t) \tag{3}$$

in which x, y, and z are dimensionless concentrations of $HBrO_2$ (activator), Br^- (inhibitor), and Ru $(bpy)_3^{3+}$ (oxidized catalyst), respectively. Parameters ϵ_1, ϵ_2, q, and h are those in the classical three-variable Oregonator [16]. The parameter y_0 denotes the dimensionless concentration of Br^- in the flow of substrates. The parameters p_1 and p_2, respectively, represent the ratio of the photochemical production of inhibitor and activator over the total photochemical reaction rate. They are fixed as follows: $\epsilon_1=0.429$, $\epsilon_2=2.319\times10^{-3}$, $q=9.5234\times10^{-5}$, $\kappa_f=1.05\times10^{-3}$, $h=0.5$, $y_0=47.619$; $p_1=0.11185$ and $p_2=0.6890$ [11]. The function $\Phi(t)$ stands for the illumination intensity varying with time t. When $\Phi(t)$ is a constant Φ_0, this system shows subcritical Hopf bifurcation when $\Phi_0=9.00\times10^{-4}$.

Here we care how an oscillatory system reacts to a linear delayed feedback applied to the external illumination intensity with the concentration of oxidized catalyst $z(t-\tau)$, in which τ is time delay. So linear delayed feedback is introduced:

$$\Phi(t) = \Phi_0 + cz(t-\tau), \tag{4}$$

where c is the strength of delayed feedback control.

III. LINEAR STABILITY

The system has a unique stationary state $\mathbf{X}_0=(x_0,y_0,z_0)$, which changes with Φ_0 and c. After linearizing the equations in the vicinity of the fixed point $\mathbf{X}_0$, the Jacobian matrix $\mathbf{J}$ can be acquired as follows:

$$\begin{pmatrix} \frac{1-2x_0-y_0-\epsilon_1\kappa_f}{\epsilon_1} & \frac{q-x_0}{\epsilon_1} & \frac{p_2ce^{-\lambda\tau}}{\epsilon_1} \\ \frac{-y_0}{\epsilon_2} & \frac{-q-x_0-\epsilon_2\kappa_f}{\epsilon_2} & \frac{2h+p_1ce^{-\lambda\tau}}{\epsilon_2} \\ 1 & 0 & -1-\kappa_f+\left(\frac{p_1}{2}+p_2\right)ce^{-\lambda\tau} \end{pmatrix}$$

and the eigenvalue problem is $\lambda\mathbf{X}=\mathbf{J}\cdot\mathbf{X}$, where $\mathbf{X}$ is the eigenvector of perturbations. The eigenvalue equation is as follows:

$$\det|\mathbf{J}-\lambda\mathbf{I}| = 0. \tag{5}$$

When $\tau=0$ and $c=0.02$, the feedback makes the Hopf bifurcation point vary from $\Phi_0=9.00\times10^{-4}$ to $\Phi_0=8.58\times10^{-4}$.

The linear stability analysis also shows that the entrainment phenomenon of the oscillatory period T by τ in the form of a piecewise linear dependence $(\tau+\delta)/N$ $(N=1,2,3,\cdots)$ exists near the unique stationary state of the system when $\tau\neq0$. Given that the system is oscillatory, we apply $\lambda=i\omega$, where the angular frequency ω is a real parameter. Substituting it into Eq. (5) and separating the real and imaginary parts of the eigenvalue equation, we derive the imaginary part of the equation

$$\alpha(\omega)\sin\omega\tau+\beta(\omega)\cos\omega\tau=f(\omega),$$

where $\alpha(\omega)$, $\beta(\omega)$, $f(\omega)$ are all polynomials of ω. The above equation can be rewritten as

$$\sin[\omega\tau+\varphi(\omega)] = \frac{f(\omega)}{\sqrt{\alpha^2(\omega)+\beta^2(\omega)}}.$$

We can simplify the above equation as

$$\sin[\omega\tau+\varphi(\omega)] = \sin(\psi(\omega)).$$

Thus its solution is

$$\omega\left(\tau+\frac{\varphi(\omega)-\psi(\omega)}{\omega}\right) = 2\pi N.$$

Since the oscillatory period of the system $T=2\pi/\omega$, we get the linear relation between T and τ:

$$T = \frac{2\pi}{\omega} = \frac{[\tau+\delta(\omega)]}{N}. \tag{6}$$

Although the dependence that δ has on ω is too complex to be simplified via approximation, numerical calculation shows that $\delta(\omega)$ is negligible compared with τ and no obvious dependent relation between δ and ω can be found. In contrast, the following simulation results show us how δ depends on the parameters.

IV. SIMULATION RESULTS

Using a constant time step $\Delta t=0.005$, we adopt the fourth-order Runge-Kutta algorithm to integrate Eqs. (1)–(3). Under delayed feedback, the system shows a variety of dynamic behaviors. Figure 1 gives us four typical oscillations of the variable $z(t)$ and the corresponding illumination $\Phi(t)$ under different parameters. Figure 1(a) shows the regular pulses. If comparing $z(t)$ with $\Phi(t)$, one can notice that in $\tau=78$ time units after a pulse in $z(t)$, $\Phi(t)$ gives a quite large change and then the system outputs the next pulse 3.9 time units later. To a certain region of time delay, such regular

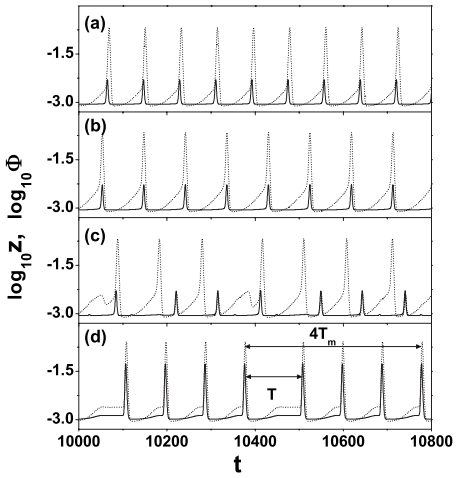

FIG. 1. Time variations of $z(t)$ (dot lines) and the corresponding illumination intensity $\Phi(t)$ (solid lines) at different parameters, (a) $\tau=78$, $c=0.02$, $\Phi_0=8.5\times10^{-4}$ in the entrainment region; (b) $\tau=94$, $c=0.02$, $\Phi_0=8.5\times10^{-4}$, where two of them synchronize completely in phase; (c) $\tau=132.5$, $c=0.02$, $\Phi_0=8.5\times10^{-4}$, where out of synchronization and in the regime of quasiperiodic motion; (d) $\tau=400$, $c=0.2$, $\Phi_0=8.5\times10^{-4}$ the system output group pulses.

pulses with no tails have the same phase trajectories in the x-z phase plane. Figure 1(b) illustrates synchronization completely in phase between the two time series. In Fig. 1(c), the quasiperiodic state emerges and there are one or two tail peaks after a major pulse. At last, Fig. 1(d) shows groups of pulses. Thus we define the interval between two adjacent pulses as T and the mean period of group pulses as T_m, respectively. For regular pulses, $T_m=T$.

Figure 2 shows the bifurcation diagram in the Φ_0-c plane. According to the different relationship between T_m and τ, the Φ_0-c plane can be divided into four regions. A linear stability analysis shows that the feedback without delay ($\tau=0$) changes the Hopf point, plotted in dots. The line dividing regions I and II is the simulation result which is quite consistent with the dotted one, i.e., the theoretical result. So

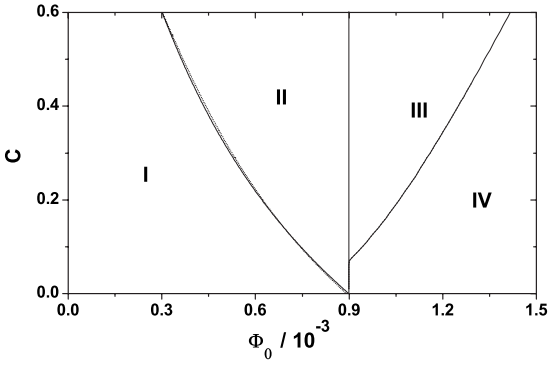

FIG. 2. Phase diagram in the parameter space of Φ_0 and feedback strength c. Region I is a region that the system has its own characteristic period T_0. The Dotted line between region I and II is the theoretical solution of Eq. (5) with $\tau=0$. Region II the system shows no immanent oscillatory period. Regions II and III are separated by the Hopf point. In region IV the system is in the state of oscillation death.

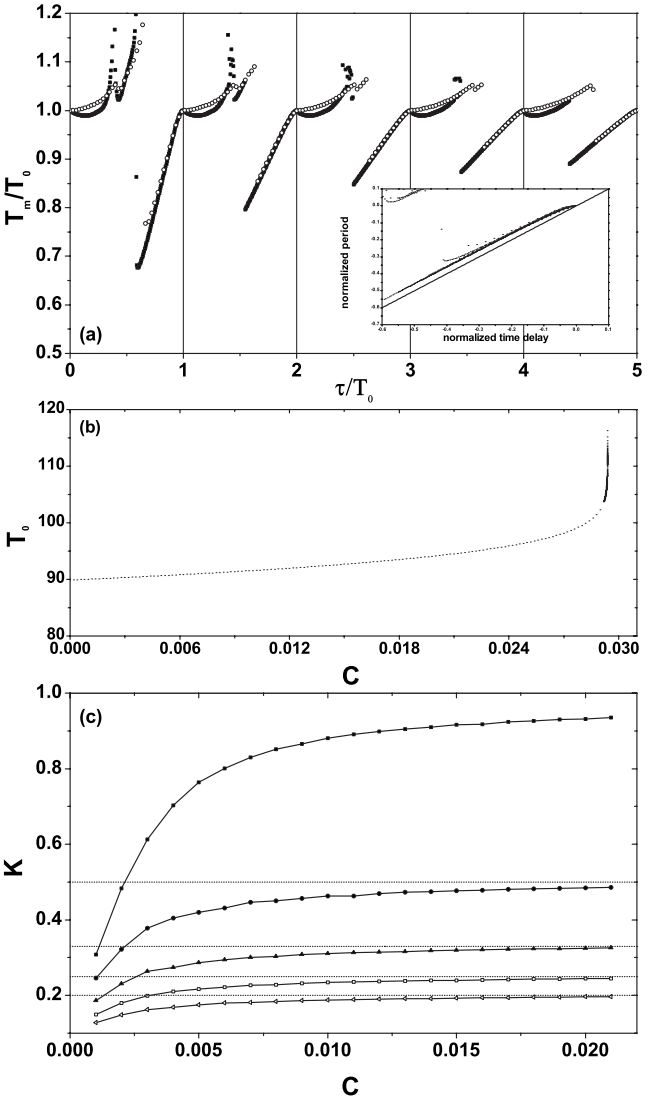

FIG. 3. (a) The relation between T_m/T_0 and τ/T_0. The solid squares are at $\Phi_0=8.5\times10^{-4}$, $c=0.02$, and the circles are at $\Phi_0=4.5\times10^{-4}$, $c=0.03$. Inset: normalized mean period versus normalized time delay, line $T_m=\tau$ is plotted for guiding eyes. (b) The characteristic period T_0 versus c at $\Phi_0=8.5\times10^{-4}$. (c) The linearly fitted slope in entrainment regions versus feedback strength c at $\Phi_0=8.5\times10^{-4}$.

under feedback without delay, in region I the system has a characteristic oscillatory period defined as T_0 while in region II the system is not oscillatory. Moreover, our simulation indicates that regions II and III are separated by the Hopf point when $c=0$. In region IV the system is in the state of oscillation death, i.e., under any delay no oscillatory state can be observed.

Figure 3(a) illustrates the variation of T_m/T_0 with τ/T_0 in region I. Interestingly, when τ increases, the variation of the mean period of the oscillations in the system repeats in T_0. Moreover, when τ is less than NT_0, delayed feedback can control the oscillatory behavior of the system [the typical dynamical behavior is shown in Fig. 1(a)] and the time delay determines the oscillatory period, in other words, the time delay entrains the oscillation of the system. When $\tau=NT_0$,

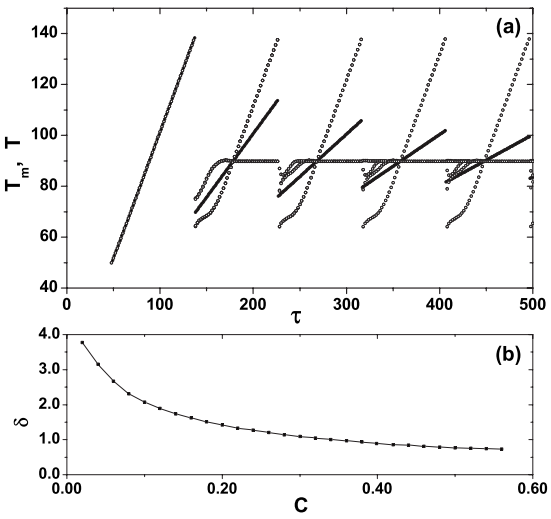

FIG. 4. (a) Typical dynamic behavior in region II. The mean period T_m(dots) and the interval between two adjacent pulses T (circles) versus time delay τ when $c=0.2$, $\Phi_0=8.5\times10^{-4}$. (b) In region II, δ versus c at $\Phi_0=8.5\times10^{-4}$.

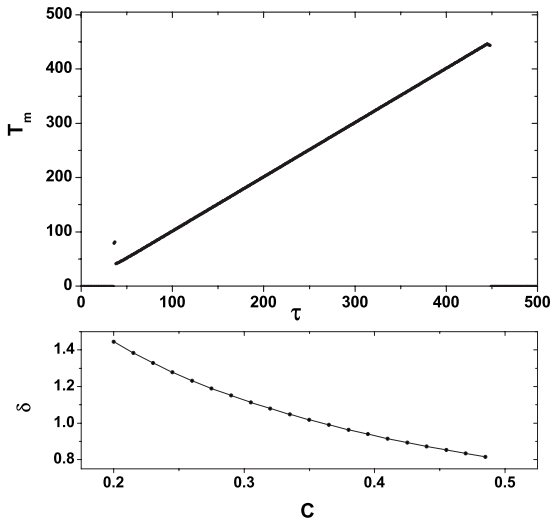

FIG. 5. (a) Typical dynamic behavior in region III. The mean period T_m versus time delay τ when $c=0.2$, $\Phi_0=9.5\times10^{-4}$. (b) In region III, δ versus c at $\Phi_0=9.5\times10^{-4}$.

Fig. 1(b) demonstrates the pulses of the system with the characteristic T_0. When $\tau>NT_0$, no clear variation of T_m with τ can be seen and the system can output nonuniform pulses as well. Figure 1(c) gives us an example of such quasiperiodic behavior.

If we focus on the entrainment regions, after applying the normalized operation, i.e., shifting the data (X,Y) in $(N-1,N]$ to $[X-N,N(Y-1)]$, and the interesting thing is that these data, which are under different parameters, lie almost in a line in the entrainment region, plotted in the inset of Fig. 3(a). Thus, we can conclude that the entrainment phenomenon is quite robust. The asymptotic line is

$$T_m = \frac{\tau + T_0\delta_0}{N}, \tag{7}$$

where $\delta_0=0.042$ is a constant while T_0 increases with increasing Φ_0 and c as shown in Fig. 3(b). On the other hand, such a robust entrainment phenomenon happens when the coupled strength c is strong enough for different Φ_0. Our simulation results show that, with increasing c, the entrainment data are gradually close to the fitted line (7). Figure 3(c) plots the linearly fitted data of the slope K in the entrainment region when c increases. It can be seen that when the system approaches the bifurcation line, the delayed feedback asymptotically entrains the oscillation of the system in the form of $T_m \propto \tau/N$. During this process, the entrainment region $(\tau<NT_0)$ expands and the nonentrainment region $(\tau>NT_0)$ with long delay becomes more irregular, especially next to the bifurcation line dividing regions I and II. Moreover, in the nonentrainment region, more quasiperiodic behaviors as shown in Fig. 1(c) can be seen with varying τ.

When the system crosses the bifurcation line and comes into region II, the oscillatory system outputs no pulses when $\tau=0$, i.e., T_0 does not exist any more. However, when τ is long enough, the dead system can be oscillatory and the entrainment phenomenon can be seen. Figure 4(a) sets an example when $\Phi_0=8.50\times10^{-4}$. One can see that the time scale of the system becomes completely determined by the time delay τ, illustrated in dots and the linear relation $T_m=(\tau+\delta)/N$ is perfectly satisfied, where δ decreases with increasing c [shown in Fig. 4(b)] but is independent from Φ_0. In Fig. 4, we also plotted the relation between T and time delay τ (in circles) and determined that the system outputs groups of pulses. For example, for $N=3$, groups are composed of three pulses each of which may have a different interval as shown in Fig. 1(d)

At last, when $\Phi_0>9.00\times10^{-4}$ for any c, the entrainment phenomenon does not appear in a sawtooth fashion. In this case, there is no distinction between T and T_m, or rather the system uniformly outputs regular pulses. In addition, the period of oscillation monotonous increases linearly with time delay in the entrainment region (from $\tau=38$ to $\tau=441$), which is almost unchanged with Φ_0 and c. This relationship could be described as $T=\tau+\delta$, where δ is independent from Φ_0, but monotonously decreases with increasing c. Typical dynamic behavior in region III is also shown in Fig. 5. In region IV, the feedback with any time delay cannot invoke oscillatory behaviors.

In other words, we observe four different dynamical behaviors of the system under the time delayed feedback in the Φ_0-c plane. We find that the state of the nonlinear system under feedback without delay and the original Hopf point of the system under no feedback can be used as hallmarks in predicting the dynamic behavior. When the system has no characteristic period under feedback without time delay, the time scale of the system is almost determined by the time delay τ and simultaneously the slope of the entrainment region becomes exactly $1/N$ (in region II) or 1 (in region III). The difference δ between the mean period T_m and the time delay τ is quite small and decreases with increasing c. In contrast, when the system has characteristic period T_0 under feedback without time delay in region I, the time scale of the system is probably determined by the competition between the characteristic period T_0 and time delay τ. Only when

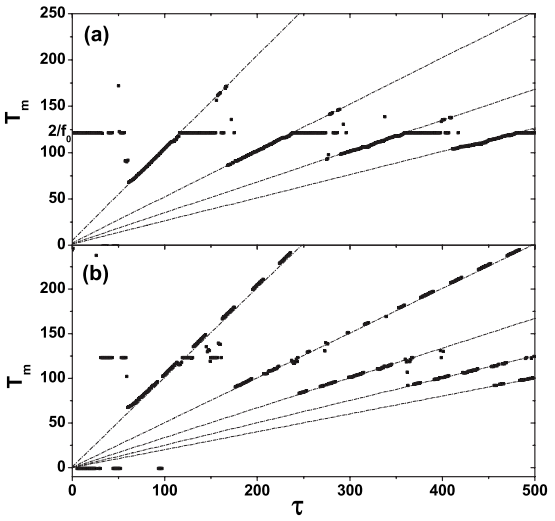

FIG. 6. Oscillation period T_m vs delay time τ for (a) $f_0=0.0165$ and (b) $f_0=0.0325$ at $c=0.02$. Dashed lines satisfy the relationship $T=(\tau+\delta_0 T_0)/N$ $(N=1,2,3,\ldots)$, where $\delta_0=0.042$ and $T_0=2/f_0$ in (a); $T_0=f_0$ in (b).

$\tau<NT_0$, the entrainment phenomenon can happen, and when c is strong enough, the entrainment data asymptotically fit the perfect linear relation (7).

To confirm our conjecture, we next consider another case of regular oscillation that the system is under the external periodic stimulus and focus on the competition between the time delay and the external period. Still using Eqs. (1)–(3), the function of illumination is chosen as follows:

$$\Phi(t) = \Phi_0 + \alpha A_m \sin(2\pi f_0 t) + c[z(t-\tau) - z(t)], \qquad (8)$$

where $\Phi_0=1.059\times10^{-3}>9.00\times10^{-4}$, $\alpha=0.965$, $A_m=0.159\times10^{-3}$. Without the feedback control $(c=0)$, previous research [12] demonstrated that the light-sensitive BZ reaction under the external period stimuli appears to be in the 1:2 phase locking state when $f_0=0.0165$ and in the chaotic state when $f_0=0.0325$. Delayed feedback in the form of $c(z_\tau-z)$ is chosen so that it does not have an influence on the subcritical Hopf bifurcation point.

Analogously, an entrainment phenomenon is triggered when we switched on the feedback loop, where $\delta_0=0.042$ reappeared, strongly indicating it to be an intrinsic value of this system (see Fig. 6). When $f_0=0.0165$, the oscillatory period is linearly determined by time delay τ in the entrainment regions and frequency locking phenomenon 1:2 is maintained in other regions. For the chaotic state $f_0=0.0325$, the system can be stabilized in a steady limit cycle by the time delayed feedback, whose characteristic period still lies near the linear lines $(\tau+\delta_0/f_0)/N$ $(N=1,2,3,\ldots)$ though not as well as in the case $f_0=0.0165$, shown in Fig. 6(b). Here we consider that, for chaotic motion, external stimuli cannot fix the system's motion in a characteristic period; thus, this causes the deviation from the fitted line, which assumes f_0 as the system's characteristic frequency.

V. DISCUSSION

Most investigations in the theory of delayed feedback are devoted to the stabilization of unstable periodic orbits embedded in chaotic attractors of low-dimensional (usually three-dimensional) systems. However, in this paper, we focus on the impact that delayed feedback has on a self-sustained oscillator and find that the dynamic behavior under the delayed feedback in global parameter space is divided into four parts. We also discovered that the state of the nonlinear photosensitive BZ system under feedback control without delay and the Hopf point can be used as hallmarks to predict the dynamic behavior. In addition to this, we observed the robust entrainment phenomena of oscillations by parametrized time delayed feedback in the photosensitive BZ reaction. It is well known that an oscillatory system either has a limit cycle with a characteristic period, or it exhibits the external period when frequency locking phenomenon happens under an external periodic stimuli. Here another kind of oscillatory mode, whose period is completely determined by delay time, is observed. From a practical point of view, the time delay can serve as the timer for the system when a time-delayed feedback loop is established.

Furthermore, when applying the time-delayed feedback loop to the Fitzhugh-Nagumo (FHN) model, which represents the activity of a neuron, we find a similar robust entrainment phenomenon. It is well established that the time delayed feedback is quite common in nonlinear dynamics of a biological system. In a recent review [17], the authors described how the recurrent discovery of circadian clock genes on *Drosophila* uncovered a molecular mechanism associated with cycling gene expression and these molecular cycles appear to emerge from delayed feedback. So we conjecture that the robust entrainment by time delay is probably a strategy to control the time scale of the system, such as the rhythm of life activities.

ACKNOWLEDGMENTS

This work was supported by the Chinese Natural Science Foundation and National Fund for Fostering Talents of Basic Science (NFFTBS), Grant No. J0630311. Wei Bao also thanks the Principal Fund of Peking University for financial support.

[1] S. Bao, J. Rihel, E. Bjes, J.-Y. Fan, and J. L. Price, J. Neurosci. **21**, 7117 (2001).
[2] M. C. Mackey and L. Glass, Science **197**, 287 (1977).
[3] G. Stegemann, A. G. Balanov, and E. Scholl, Phys. Rev. E **73**, 016203 (2006).
[4] C. Beta, M. Bertram, A. S. Mikhailov, H. H. Rotermund, and G. Ertl, Phys. Rev. E **67**, 046224 (2003).
[5] T. Chevaliar, A. Freund, and J. Ross, J. Chem. Phys. **95**, 308 (1991); P. W. Roesky, S. I. Doumbouys, and F. W. Schneider, J. Phys. Chem. **97**, 398 (1993).
[6] K. Sriram, Chaos, Solitons Fractals **28**, 1055 (2006).
[7] O. U. Kheowan, V. S. Zykov, O. Rangsiman, and S. C. Müller, Phys. Rev. Lett. **86**, 2170 (2001).
[8] Lu-Qun Zhou, Iris Cassidy, S. C. Müller, Xi Cheng, Guan Huang, and Qi Ouyang, Phys. Rev. Lett. **94**, 128301 (2005).
[9] S. Kádár, T. Amemiya, and K. Showalter, J. Phys. Chem. A **101**, 8200 (1997).
[10] T. Amemiya *et al.*, J. Phys. Chem. A **102**, 4537 (1998); **103**, 3451 (1999).
[11] P. Parmananda, H. Mahara, T. Amemiya, and T. Yamaguchi, Phys. Rev. Lett. **87**, 238302 (2001).
[12] H. Mahara *et al.*, Physica D **205**, 275 (2005).
[13] N. B. Janson, A. G. Balanov, and E. Schöll, Phys. Rev. Lett. **93**, 010601 (2004).
[14] A. G. Balanov, V. Beato, N. B. Janson, H. Engel, and E. Scholl, Phys. Rev. E **74**, 016214 (2006).
[15] J. Weiner, F. W. Schneider, and K. Bar-Eli, J. Phys. Chem. **93**, 2704 (1989).
[16] R. J. Field, *Oscillations and Traveling Waves in the Chemical System*, edited by M. Burger (Wiley, New York, 1984).
[17] P. Meyer and M. W. Young, J. Biol. Rhythms **22**, 283 (2007).